Hindawi
Journal of Nanomaterials
Volume 2017, Article ID 4838095, 13 pages
https://doi.org/10.1155/2017/4838095

Research Article

Dielectric and Electrical Properties of WS_2 Nanotubes/Epoxy Composites and Their Use for Stress Monitoring of Structures

A. Sedova,[1,2] S. Khodorov,[2] D. Ehre,[2] B. Achrai,[2] H. D. Wagner,[2] R. Tenne,[2] H. Dodiuk,[1] and S. Kenig[1]

[1] *Shenkar College of Engineering and Design, 52526 Ramat Gan, Israel*
[2] *Department of Materials and Interfaces, Weizmann Institute of Science, 76100 Rehovot, Israel*

Correspondence should be addressed to S. Kenig; samkenig@shenkar.ac.il

Received 31 October 2016; Revised 13 January 2017; Accepted 6 April 2017; Published 4 May 2017

Academic Editor: Zafar Iqbal

The dielectric and electrical characteristics of the semiconductive WS_2 nanotubes/epoxy composites were studied as a function of the nanotubes concentration and the pressure applied during their molding. In addition, the ability of WS_2 nanotubes to serve as stress sensors in epoxy based nanocomposites, for health-monitoring applications, was studied. The nanocomposite elements were loaded in three-point bending configuration. The direct current was monitored simultaneously with stress-strain measurements. It was found that, in nanocomposites, above the percolation concentrations of the nanotubes, the electrical conductivity increases considerably with the applied load and hence WS_2 nanotubes can be potentially used as sensors for health monitoring of structural components.

1. Introduction

The ability to detect damage in structures before failure is a critical issue. Hence, various structural health-monitoring systems were developed for aerospace [1, 2] and civil infrastructures [3]. The interest for incorporating nanoparticles in polymers has grown in the last two decades. Various nanofillers offer wide range of properties such as mechanical [4], thermal [5], and electrical [6] conductivities and may be successfully introduced into polymers [7–10]. Since their discovery, carbon nanotubes (CNTs) [11, 12] were investigated intensively and a wide range of applications were offered to various devices based on CNTs. One of the main features of this nanomaterial is its high electrical conductivity [6]. Due to their high electrical conductivity CNTs-based nanoelectromechanical devices were developed and described [13]. The ability of the CNTs to respond electrically to the applied external load [14, 15] led to the development of sensors, which can be inserted into structural elements and serve as nanosensors for structural health monitoring [16–18]. It was shown that the main mechanism responsible for the resistance change in the CNTs/polymer stress sensing systems is the tunneling effect, which is strongly dependent on the nanotube-nanotube distance [19, 20].

Inorganic nanotubes (INT) and fullerene-like nanostructures (IF) of tungsten and molybdenum disulfide were discovered in 1992 [21] and 1993 [22], respectively. The mechanical properties of individual WS_2 nanotubes have been investigated in some detail [4, 23]. The Young's modulus was found to be 160 GPa and the ultimate strength of the nanotubes between 6 and 21 GPa. It was found that the addition of minute amounts (<2 wt.%) of nanotubes to polymer matrices [7–9], and in particular to epoxy resin, enhances the mechanical properties of the nanocomposite. However, beyond a critical concentration of 0.5 wt.%, the mechanical properties of the resin deteriorate [8].

The semiconducting properties of individual WS_2 nanotubes were also investigated [24–26]. Inorganic nanotubes of WS_2 (INT-WS_2) showed a high conductivity (in vacuum conditions) [25]. Moreover, it has been established that applying an external force on single INT-WS_2 (torsion or tension) results in increased conductivity, due to a piezoelectric effect

[26]. Recently, low-temperature quasi-1D superconductivity was demonstrated for a WS_2 nanotube gated with an ionic liquid [27]. Theoretical study based on the density functional method indicated the band structure-strain relation for single W/MoS_2 nanotubes [24]. It was shown that applying tensile force on the nanotube leads to elongation of the W/Mo-S bonds resulting in shrinkage of the nanotube bandgap. Thus, in the case of electromechanical devices based on such nanotubes and in great contrast with CNT, higher electrical conductivity response is expected upon application of a tensile force.

The influences of INT-WS_2 on the mechanical, tribological, and thermal performance of thermoplastic [28] as well as thermosetting [8, 29, 30] polymeric matrices were reported in the literature. Nevertheless, only little work has been devoted to the electrical conductivity of polymers containing INT-WS_2 [31, 32].

It was shown that the presence of CNTs in a polymeric matrix such as poly(vinylidene fluoride) (PVDF) [33, 34] and polycarbonate (PC) [35] influences the dielectric properties of the polymers. It was also observed that the conductivity, dielectric constant, and the dielectric loss increase with higher content of the nanotubes. In addition, the dispersion technique [35] and surface functionalization [33] of the CNTs was shown to influence their dielectric behavior. The dielectric properties of INT-WS_2, incorporated in vinylidene fluoride-co-hexafluoropropene (PVDF-HFP) nanofiber have been analyzed as well [36]. Recently, DC conductivity and the dielectric properties of the CNTs/INT-WS_2 hybrid films have been presented [37].

Generally speaking, multiwall carbon nanotubes possess mainly metallic character [6] and therefore their conductivity is appreciably higher than that of multiwall WS_2 nanotubes. The percolation threshold of CNT varies with different parameters and is generally up to 1 wt.%. In general, due to increasing nanotube-nanotube distance, CNT-embedded in polymer matrices show reduced conductivity upon application of a tensile force [16–18]. Being semiconductors, the reaction of WS_2 nanotubes to an applied tensile force is expected to be palpably larger than that of CNT and in opposite direction. Therefore, in contrast to CNT-polymer composite, the application of a tensile force on INT-WS_2 nanotubes-polymer composite leads to a reduced resistivity. The special gravity of WS_2 nanotubes (about 5000 kg/m^3) is appreciably higher than that of carbon nanotubes (ca. 1500 kg/m^3). Consequently, weight-wise, much higher WS_2 nanotubes content is required for achieving percolation in polymer nanocomposites, compared to CNT. In summary, INT-WS_2 should be suitable for stress sensing in polymer matrices, but at higher content than that used for CNT, which is the topic of the present work. Obviously, though, the addition of WS_2 nanotubes to a polymer beyond say 2 wt.% is likely to adversely influence the mechanical properties of the matrix. Hence, WS_2 nanotubes-based health-monitoring devices should be placed in confined space in the construction module, in order to minimize the mechanical shortcomings of high concentrations of WS_2 nanotubes.

Ohm's Law (1) describes the direct current (DC), voltage, and resistance relationship [38, 39]. In this case, the material is an ideal resistor responding to an applied external voltage (U) and a uniform current flow (I) is detected. The measured samples resistance (R) is described using

$$R = \frac{U}{I}, \tag{1}$$

$$R = \rho \cdot \frac{L}{A}, \tag{2}$$

where ρ [ohm cm] is the electrical resistivity, L is the length of the sample, and A is the cross-section area. The electrical conductivity of the sample is defined as the inverse value of the resistivity.

Impedance is the complex resistance, where the measured samples are represented by an equivalent circuit consisting of a network of resistors, capacitors, and inductors connected in series and in parallel [39, 40]. The impedance is represented as a complex number composed of a "real" (in-phase) ($Z_{\mathrm{REAL}(\omega)}$) and "imaginary" (out-of-phase) ($Z_{\mathrm{IM}(\omega)}$) parts

$$Z^* = Z_{\mathrm{REAL}(\omega)} + jZ_{\mathrm{IM}(\omega)}. \tag{3}$$

For the simple case, where the sample is described as an electronic circuit consisting of ideal resistor and ideal capacitor connected in parallel, Z^* is calculated using

$$Z^* = \frac{R}{1 + (\omega RC)^2} + j\frac{\omega R^2 C}{1 + (\omega RC)^2}, \tag{4}$$

where C is the capacitance and ω is the frequency defined by the applied AC (alternating current) frequency $f, \omega = 2\pi f$.

The phase angle (ϕ) is the ratio between the two parts

$$\tan\phi = \frac{Z_{\mathrm{IM}}}{Z_{\mathrm{REAL}}}. \tag{5}$$

The complex plane impedance diagram, also known as "Nyquist plot," is obtained by relating Z_{REAL} (x-axis) and Z_{IM} (y-axis). At low frequencies the impedance shows completely resistive behavior (right side of the plot), while at high frequencies the impedance is dominated by the capacitive element (left side of the plot).

Impedance analysis carried out by AC potential modulation provides information such as material permittivity (ε^*) and conductivity (σ).

Similar to the complex impedance, the material permittivity (ε^*) is a complex number, consisting of the "real" (ε'-permittivity or dielectric constant) and the imaginary (ε''-imaginary permittivity or loss factor) parts [39]

$$\varepsilon^* = \varepsilon' + j\varepsilon'' = \frac{CL}{\varepsilon_0 A} + j\frac{L}{RA\omega\varepsilon_0}, \tag{6}$$

where $\varepsilon_0 = 8.85 \cdot 10^{-14}$ [F/cm] is the electrical permittivity in vacuum.

In this work the electrical behavior of a composite consisting of INT-WS_2 incorporated in epoxy polymer matrix was studied under an applied load. Three-point bending configuration was used for the study. During the measurements, the direct current and the stress-strain relationship of the

INT-WS_2/epoxy composites were monitored simultaneously. DC electrical conductivity and the dielectric behavior of the composites were analyzed using *I-U* and impedance characterizations, respectively, with the goal of investigating the possibility of using INT-WS_2 in polymer composites as stress sensors for health monitoring of structures. In order to have sufficient sensitivity the concentration range of the nanotubes was appreciably higher (up to 25 Vol.%) than that used for improving the mechanical properties of the epoxy resin. Consequently, the overall mechanical behavior of the presently studied nanocomposites was inferior to that of the pure epoxy.

2. Experimental

2.1. Materials. WS_2 nanotubes (INT-WS_2) were purchased from NanoMaterials Ltd. (Israel). The diameter and length of the nanotubes were 50–120 nm and 1–20 μm, respectively [41, 42]. The epoxy resin used was based on di-glycidyl ether of bisphenol-A (DGEBA) (DER 331 product of Dow Chemical, Midland, MI, USA). The curing agent was polyetheramine (JEFFAMINE® T-403, product of Huntsman) with theoretical equivalent weight of 81. High purity silver paint (SPI Supplies, USA) was used to establish the electric contacts.

2.2. Samples Preparation. Two families of INT-WS_2/epoxy composite samples were prepared, each one serving for different set of experiments. The first family of composites contained various contents 0.22, 0.66, 1.1, 2.2, 3.2, and 6.2 Vol.% of the INT-WS_2, samples 1–6, respectively.

This series of samples was used to study the percolation threshold of the nanotubes-epoxy resin composites. These samples were prepared without the application of compressing pressure. Due to the viscous nature of the epoxy-nanotube mixture, a concentration above 6.2 Vol.% was not accessible according to the present technique. The influence of the nanotubes concentration on the formation of the percolating network was studied using impedance characterization.

The second family consisted of samples containing high volume fraction (25 Vol.%) of the INT-WS_2 (samples 7–11). Sample 7 was prepared by careful mixing of the nanotubes in the epoxy resin and consequently the nanotubes were relatively well dispersed in the epoxy resin. This sample was prepared in order to study the influence of mixing of the insulating polymer and the INT-WS_2 on its' overall DC conductivity and the dielectric properties.

On the other hand, samples 8–11 were mixed only lightly but were prepared under an applied pressure. Hence, the nanotubes were heavily aggregated in these samples, which, inevitably led to poor mechanical integrity of the samples. The concentration of the nanotubes in these samples is beyond the percolation threshold and accordingly meaningful DC conductivity and impedance analysis could be obtained. This set of samples was used for studying the electrical response of the INT-WS_2 under applied load concomitant with the stress-strain relationship (for potential health-monitoring purposes). For the preparation of samples 8–11 various compressing pressures (0.8, 13.9, 27.8, and 55.6 MPa) were used. The influence of the various compressing pressures on the electrical behavior of the composites samples was evaluated. It was found that concentration of 25 Vol.% of the nanotubes is optimal for the samples prepared using that technique. Specimens with lower nanotubes content were not sufficiently viscous. Therefore, the fluid escaped out of the mold under the applied pressure making sample preparation close to impossible. The majority of the results concerning these samples are reported in the Supplementary Information (in Supplementary Material available online at https://doi.org/10.1155/2017/4838095).

2.2.1. Preparation of Composites Containing Low Volume Fraction of the INT-WS_2 (Samples 1–6). Preformed consolidated INT-WS_2 material was dispersed in the curing agent phase (JEFFAMINE T-403) by sonication of 4 min (3 times) using ultrasonic bath (MRC, AC-120H, operated at frequency of 50 Hz). This was followed by mechanical mixing, using a spatula. Another 4 min of sonication of the JEFFAMINE/INT-WS_2 mixture was carried out using a high intensity probe sonicator (tip diameter 19 mm) with response frequency of 20 kHz ± 50 Hz (VCX 400-ultrasonic processor and CV26 tip, Sonics & Materials, Inc., vibra-cell, USA). Then, the JEFFAMINE/INT-WS_2 mixture was blended with the epoxy resin (30 : 70 w/w) and degassed for 30 min. Finally, the samples curing was carried out in the RTV molds.

To allow the residual bubbles getting out of the resin mixture it was left at ambient conditions for 1 hr. Subsequently, the samples were heated for 3.5 and 2.5 hours at temperatures of 40°C and 80°C, respectively, for the curing process. Samples with thickness, width, and length of 1.5±0.3, 4.1 ± 0.14, and 9.1 ± 0.6 mm, respectively, were thus prepared.

In addition to the samples consisting of a nanotube-epoxy mixture in different proportions, pellets consisting of pure nanotubes were prepared for a reference by applying a pressure of 980 MPa on the INT-WS_2 powder. The dimensions of the prepared pellets were surface area 20 ± 0.08 mm^2 and thickness 0.62 ± 0.03 mm.

2.2.2. Preparation of Composites Containing High Volume Fraction of the INT-WS_2 (Samples 7–11). Samples containing a high volume fraction of INT-WS_2 (25 Vol.%) were prepared by mixing the nanotubes with epoxy resin premixed with the curing agent and degassed for 30 min. The matrix and the INT-WS_2 densities were 1160 kg/m^3 [43] and 5000 kg/m^3 (taking into account the empty core of the INT-WS_2), respectively. The pristine INT aggregates (20–90 μm) were dried at 120°C for 3 h (in vacuum) before mixing with the epoxy.

In the first step of preparation of the nanocomposites, the INT-WS_2 powder was lightly mixed using spatula for 1 min with the epoxy resin, in order to wet the aggregates' surfaces by the polymer. This treatment produced a consolidated material, which could be further molded to any shape. After the mixing a wet compound was obtained consisting of INT-WS_2 encapsulated by the epoxy (Figure 1). For the samples fabrication, specially designed mold (Figure 2(a)) was used. The mold permitted the compression of the INT-WS_2/epoxy mixture before curing. To prevent the epoxy from sticking to the mold walls during the compression, Teflon spacers were used. Four compressing pressures of 0.8, 13.9, 27.8, and

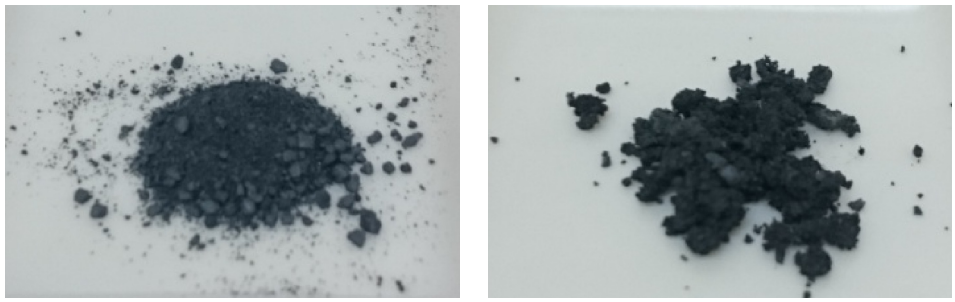

(a) (b)

Figure 1: INT-WS_2 powder (a) before and (b) after mixing with slight amount of the epoxy resin.

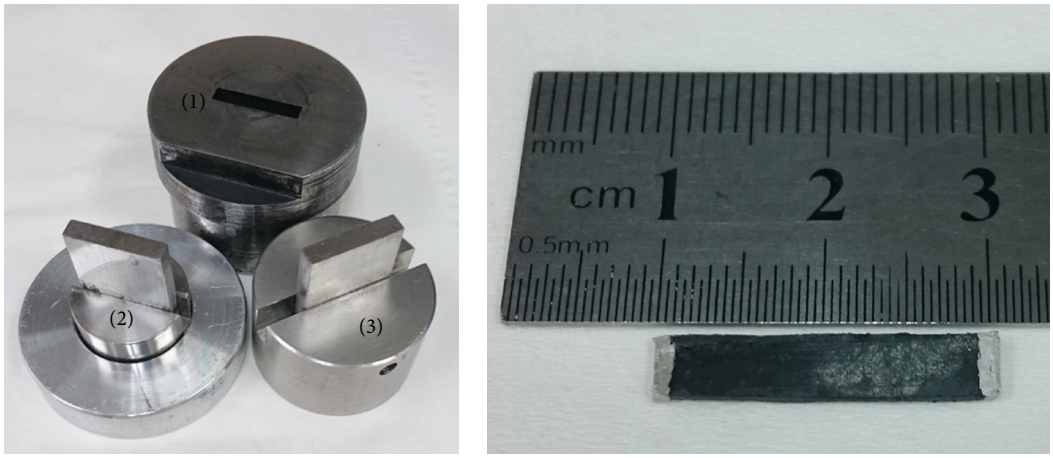

(a) (b)

Figure 2: Mold for samples preparation: (a) (1) mold body and (2) lower movable part which is inserted to the cavity during compression. This device configuration allows the samples ejection after the compression. (3) Upper movable part, encountering the compressing pressure (device assembly is shown in the Supplementary Information Fig. S3). (b) Samples configuration for the three-point bending test.

55.6 MPa were applied; samples were marked as 8 to 11, respectively. After compression the samples were transferred to silicone (room temperature vulcanized (RTV)) molds for the curing process. High purity silver paste was applied on the sample surface to establish electrical contacts (Figure 2(b)).

In addition, samples with thoroughly mixed INT-WS_2 and the epoxy were prepared as a kind of reference without using the compression mold (sample 7). To achieve a more uniform mixing and partial deagglomeration of the nanotubes in the epoxy resin, the nanotube powder was mechanically mixed with the polymer resin (using spatula) for 5 min. The better mixing (compared to samples 8–11) of the INT-WS_2 with the epoxy allowed us to achieve material which could be cast into the RTV mold. Samples dimensions are given in Table 1.

2.3. Impedance Measurements. The dielectric properties measurements were performed using high resolution dielectric analyzer (HRDA) (Novocontrol Technologies). For the samples containing various Vol.% of the nanotubes (samples 1–6) and samples 7–11, the AC voltage was set to 1 V. For the pure INT-WS_2 pellets the applied AC voltage was 0.1 V, in order to prevent high currents during the measurements. The AC measurements were carried out without applying DC voltage (zero bias) in the frequency range of 10^1–10^6 Hz.

2.4. Measurement Set-Up for Stress Monitoring in Composites. In order to study the electrical response due to the applied load, a three-point bending configuration was used (Supplementary Information Fig. S1). Three-point bending tests were performed using a mechanical loading system (Bose® ElectroForce® 3220) with a load cell of 225 N. Samples 8–11 were loaded at a rate of 0.0005 mm/s.

I-U measurements and the time dependence of the current were monitored under the applied load (Precision Source/Measure Unit, KEYSIGHT B2912A). The applied DC voltage was set to 50 V. Before applying the load, the measured current was varying slightly with time. The resistance (conductivity) stabilized only after 1.3–5 min. The load was applied once a relatively constant conductivity region was reached (Supplementary Information Fig. S2). Upon applying the load

Table 1: Samples dimensions and measured average DC conductivities. Sample 7 contained 25 Vol.% of INT-WS_2 which were mixed thoroughly with the epoxy resin without compression (cast only). Samples 8–11 containing 25 Vol.% of nanotubes were only lightly mixed and were compressed by applying pressures of 0.8 (sample 8), 13.9 (sample 9), 27.8 (sample 10), and 55.6 (sample 11) MPa.

Sample type	Length [mm]	Width [mm]	Thickness [mm]	σ [S/m]
Neat epoxy	20.00 ± 0.05	4.10 ± 0.03	1.46 ± 0.05	$2.3 \cdot 10^{-10} \pm 2.2 \cdot 10^{-10}$
Pellet-neat INT-WS_2	—	—	0.62 ± 0.03	$1.2 \cdot 10^{-1} \pm 3.2 \cdot 10^{-3}$
Sample 7	22.10 ± 0.03	4.30 ± 0.01	1.04 ± 0.06	$1.9 \cdot 10^{-7} \pm 3.44 \cdot 10^{-9}$
Sample 8	20.40 ± 0.05	4.30 ± 0.07	1.18 ± 0.08	$3.3 \cdot 10^{-5} \pm 8.1 \cdot 10^{-6}$
Sample 9	20.60 ± 0.02	4.34 ± 0.07	1.01 ± 0.06	$2.3 \cdot 10^{-5} \pm 4.6 \cdot 10^{-6}$
Sample 10	20.50 ± 0.02	4.40 ± 0.06	0.98 ± 0.05	$2.8 \cdot 10^{-5} \pm 2.4 \cdot 10^{-5}$
Sample 11	20.50 ± 0.05	4.37 ± 0.05	0.88 ± 0.08	$2.7 \cdot 10^{-5} \pm 1.2 \cdot 10^{-5}$

Table 2: Average sensitivity factors, maximum current increase, and the maximum strain (at breaking point), and the samples strength.

Sample type	⟨SF⟩-test 1, strain range 0.3–0.6 [%]	⟨SF⟩-test 2, strain range 0.3–0.6 [%]	⟨SF⟩-test 3, strain range 0.3–0.6 [%]	⟨SF⟩-test 3, strain range 1.0–1.3 [%]	Maximum current increase at the breaking point [%]	Maximum strain [%]	Strength [MPa]
Neat epoxy	—	—	—	—	—	8.6	59.4
Sample 8	0.7 ± 0.1	0.5 ± 0.2	0.7 ± 0.1	2.1 ± 0.3	2.7 ± 0.6	2.0 ± 0.2	38.9 ± 1.9
Sample 9	0.3 ± 0.1	0.3 ± 0.1	0.3 ± 0.1	1.3 ± 0.2	2.0 ± 0.1	1.7 ± 0.4	42.0 ± 0.2
Sample 10	0.4 ± 0.1	0.6 ± 0.5	0.7 ± 0.5	1.2 ± 0.1	2.3 ± 0.6	1.9 ± 0.1	38.5 ± 3.3
Sample 11	0.8 ± 0.7	0.6 ± 0.1	0.7 ± 0.1	1.6 ± 0.1	2.3 ± 0.6	1.7 ± 0.3	37.8 ± 1.0

(continuously), a current increase was observed, respectively (Figure 9(b)).

The relative change in the resistance to the strain (sensitivity of a strain sensor) is described by the Gauge factor [44]. The Gauge factor, also known as a sensitivity factor (SF) [45], is calculated using

$$\mathrm{SF} = \frac{\Delta R}{R_0 \Delta \varepsilon}, \tag{7}$$

where ΔR is the resistance change due to the applied load, R_0 is the resistance for the unloaded sample, and $\Delta\varepsilon$ is the measured strain. In the present case, the electrical resistance decreased due to the applied load and consequently the electrical current was increased. Thus, the calculated sensitivity factors are multiplied by –1.

Three samples of each type (samples 8–11) were characterized. First, each sample was loaded twice (test 1-2) without reaching the breaking point, while during the third loading (test 3) the ultimate applied load led to breaking of the samples. The sensitivity factors were calculated for each test (test 1–3), for the strain range of 0.2–0.6% and for 1–1.3% for the third loading (Table 2). All loaded samples exhibited current increase due to the applied load (Figure 9(b)). The current increase was found to be more significant beyond a strain of 0.79 ± 0.13%.

2.5. Microscopy Characterization. The analysis of the nanotubes dispersion of the samples containing low volume fraction (0.22–6.2%) of the nanotubes (samples 1–6) was performed in environmental scanning electron microscope (ESEM) (model Philips XL-30). Electron microscopy examination of the fractured samples (samples 7–11) and of the compressed nanotubes' pellet was performed using a scanning electron microscope (SEM) (Carl Zeiss ULTRA 55).

3. Results and Discussion

ESEM observation of the samples containing low Vol.% of the nanotubes (0.22–3.2 Vol.%), samples 1–5 (Figure 3(a)), confirmed a good dispersion of the INT-WS_2 in the polymeric medium. It was found that only at a concentration of 6.2 Vol.% (sample 6) the nanotubes start to segregate significantly (Figure 3(b)).

As can be seen from Table 1, the application of a compression molding pressure for epoxy samples containing 25 Vol.% of the INT-WS_2 led to a reduced sample thickness. Furthermore, it can be noticed that addition of the nanotubes to the epoxy resin leads to increase of the electrical conductivity by five orders of magnitude, compared to the neat epoxy. Sample number 8, which was prepared under the lowest pressure (0.8 MPa), showed the highest conductivity among samples 7–11, while cast sample 7 (no pressure applied) exhibited the highest resistance among the samples. Nonetheless, the pure INT based pellet exhibited the highest electrical conductivity.

Due to the light mixing process of the INT-WS_2 powder with the epoxy (samples 8–11), a percolating network was obtained with a minor effect of the polymer on the electrical conductivity (Table 1). SEM images (Figure 4) showed that applying high compression pressures led to reduced distance between the granules (agglomerates) but at the same time more polymers were pushed in between them. For sample 8, the SEM analysis shows that some of the WS_2 nanotubes are bare and therefore they form direct contacts between the aggregates without significant interfering of the insulating

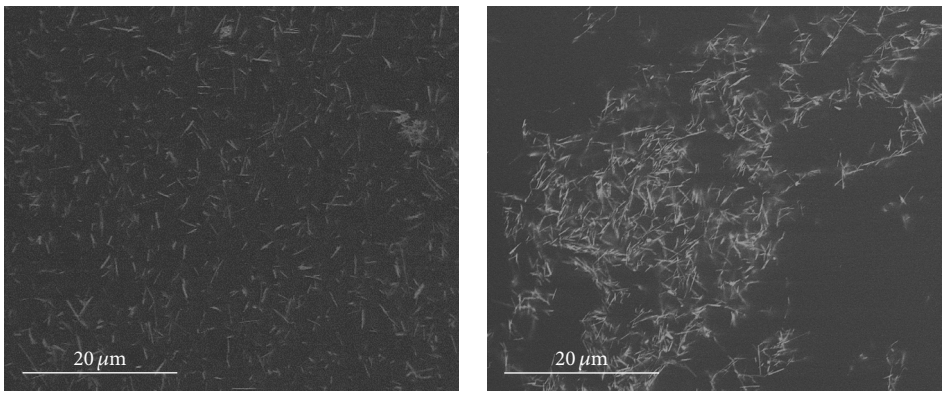

(a) (b)

Figure 3: ESEM images of the INT-WS_2 dispersed in the epoxy matrix (a) sample 4 (2.2 Vol.%) and (b) sample 6 (6.2 Vol.%).

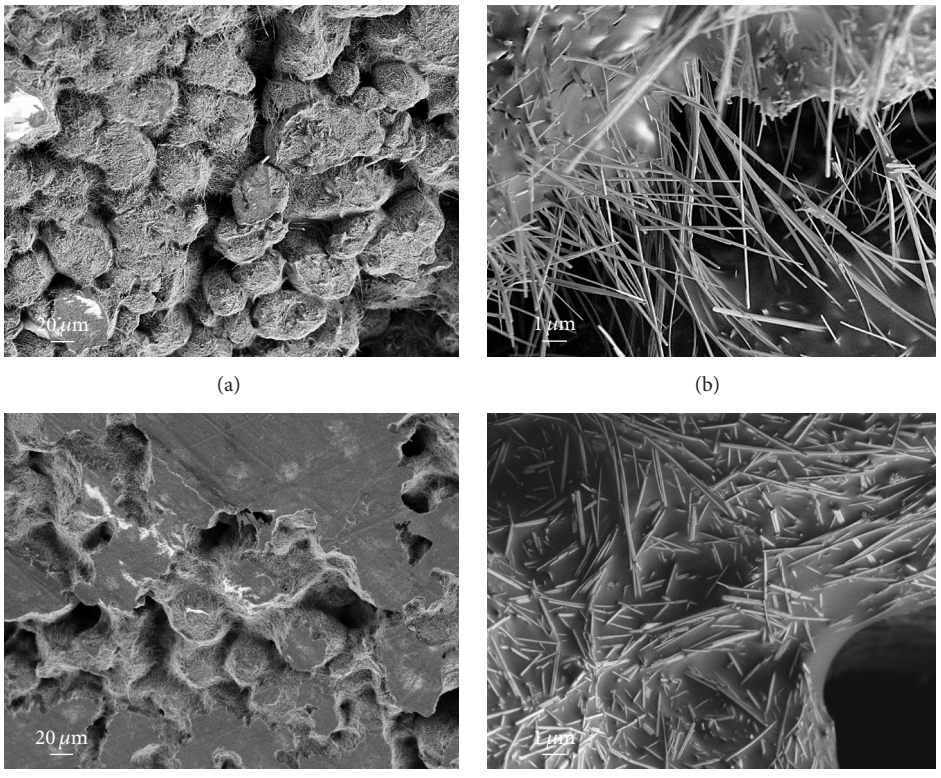

(a) (b)

(c) (d)

Figure 4: SEM images of sample 8 (prepared with a load of 0.8 MPa) (a) low and (b) high magnifications; (c) low and (d) high magnifications of sample 9 (13.9 MPa). While the nanotubes appear nude in sample 8, polymer infiltration between the tubes (and consequently electrical insulation) is obvious in sample 9.

polymer (Figure 4(b)), while, for samples 9–11, which were compressed under higher pressures, the insulating polymer was squeezed between the nanotube aggregates to a larger extent, leading to diminution of the overall conductivity of the samples (Figure 4(d)). Hence, in general the conductivity decreased with the higher applied pressure. By analyzing the fractures of samples 8–11, a weak interaction between the epoxy and the nanotubes was observed (Figure 5(a)). For sample 7, where the INT-WS_2 were well mixed with the epoxy resin, the insulating polymer wrapped the individual nanotubes (Supplementary Information Fig. S4). Consequently, this sample exhibited low conductivity values compared to samples 8–11. Here one can see that the better is the interaction between the nanotubes and the insulating

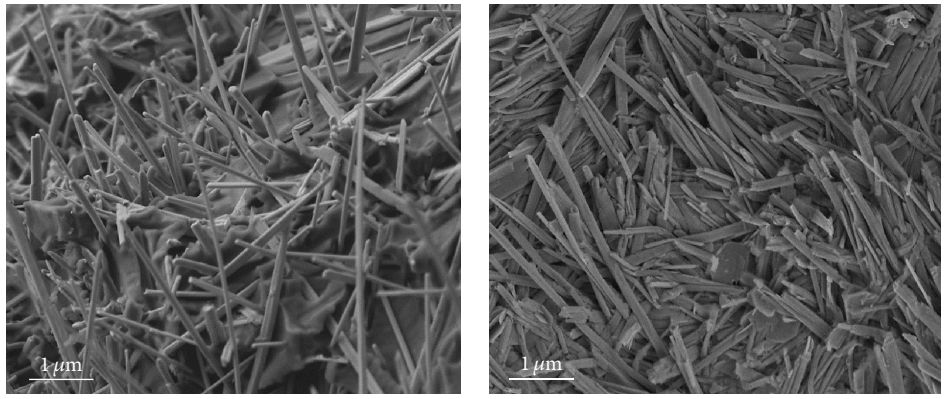

(a) (b)

Figure 5: SEM images of the fractured surface of (a) sample 10 (prepared under load of 27.8 MPa) and (b) pellet consisting of pure INT-WS_2.

polymeric matrix the lower is the DC conductivity (for the same 25 Vol.% of the nanotubes). Contrarily, the high pressure (980 MPa), which was used to prepare the pure nanotubes pellet (Figure 5(b)), secured a good interfacial contact between the nanotubes facilitating the electron transfer between the nanotubes. Thus, the contact resistance in this case was negligible and high conductivity values could be achieved (Table 1).

3.1. Impedance Analysis of the Samples. In this part, samples 1–6 with different content of the nanotubes (0.22–6.2 Vol.%), cast sample 7, and samples 8–11 prepared under different pressures (0.8–55.6 MPa) were analyzed. Samples 1–6 were used for investigating the formation of a percolating network. Epoxy composites containing INT-WS_2 present a complicated system that could be characterized using the following assumptions:

(1) R (epoxy) $\gg$ R (nanotubes).

(2) C (nanotubes) $\gg$ C (epoxy).

(3) In that case, the system response is a combination of conducting elements of INT-WS_2 (discontinuous phase) and poorly conducting elements of epoxy (continuous phase) [39, 40].

(4) Due to the semiconducting properties of the nanotubes, each nanotube is assumed to behave as an individual capacitor.

Consequently, at low concentration of the nanotubes (0.22–3.2 Vol.%, i.e., samples 1–5) the electron path is inhibited by the poorly conducting epoxy. As the volume fraction of the nanotubes increases, a percolating network is starting to form (Figure 3(b)); thus, more electrons are able to be transported through the medium. When the nanotubes create a continues percolating network (samples 8–11 with 25 Vol.%) the influence of the epoxy decreases significantly.

Nyquist plot of the pure INT-WS_2 pellet completes its semicircle at low frequencies (Figure 6(a)), while, at high frequencies the semicircle is fragmented, probably due to the system limitation to reach frequencies higher than 10^6 Hz.

For the electrically conducting samples 8–11 (25 Vol.% nanotubes) the Nyquist plots (Figure 6(b)) almost complete an ideal semicircle. It was observed that sample 8 (prepared under pressure of 0.8 MPa) presents the smallest resistive element among the studied conducting samples (8–11), which agrees with the DC current measurements (see Table 1). At the high frequencies the specimen response is dominated by the capacity of the nanotubes, while at the low frequencies range the response reflects mostly the contribution from the high resistance of the polymer [39].

Furthermore, due to the presence of the polymeric phase, the distance between individual nanotubes increased compared to the pure INT-WS_2 pellet (Figure 5) and hence the effect of the electrons tunneling between the nanotubes is suppressed in some extent. The arcs (Figure 6(b)) seem to be expanded. One reason for such a behavior could be the convergence of two separate arcs into an expanded single arc (see equivalent circuit in Supplementary Information Fig. S5) [40].

For the neat epoxy as well for sample 6 (6.2 Vol.% of the nanotubes) and sample 7 (Figure 6(c)) the impedance plots do not intersect the x-axis at high frequencies nor complete their semicircular form. This behavior can be attributed to the high resistive element of the samples.

The calculated dielectric constant-ε', the loss factor-ε'', and AC conductivity are displayed in Figure 7. This analysis indicated that the values of ε', ε'', and AC conductivity increased with the formation of the percolating network of nanotubes (samples numbers 8–11). For samples 9 and 10 the calculated values were found to be about the same; therefore, the plots for these samples are overlapping (Figure 7). Sample 7 (cast sample prepared without applied pressure) showed the lowest dielectric constant-ε', loss factor-ε'', and AC conductivity values among samples 7–11, containing 25 Vol.% of the nanotubes (Supplementary Information Fig. S6). Impedance characterization of the samples containing low weight percentages (samples 1–5, see Supplementary Information Fig. S7) demonstrated little effect of the nanotubes on the dielectric characteristics. For the sample with 6.2 Vol.% of INT-WS_2 (sample 6), where segregated nanotubes are observed

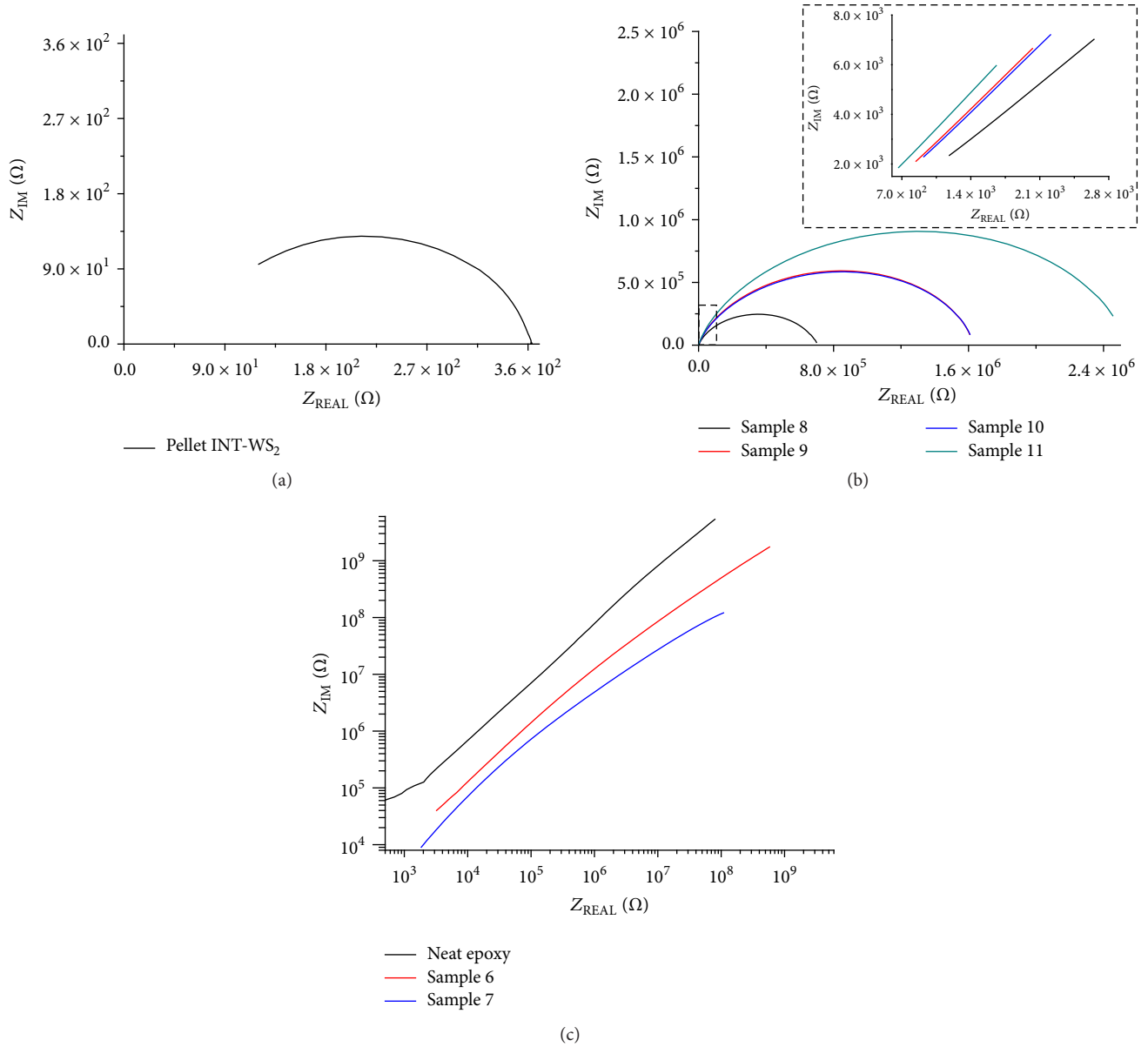

FIGURE 6: Impedance spectra of the (a) INT-WS_2 pellet; (b) samples 8–11 (with 25 Vol.% nanotubes). The inset shows the magnification of the Nyquist plots behavior at the high frequencies range. (c) The impedance spectra of the neat epoxy, sample 6 (6.2 Vol.% of nanotubes) and sample 7 (cast with 25 Vol.% of the nanotubes).

(Figure 3(b)), the calculated dielectric constant, loss factor, and DC conductivity were found to increase, compared to the neat epoxy (Figure 7).

3.2. I-U Characterization of the Samples. *I-U* measurements of the compressed pure INT-WS_2 exhibited a semiconducting behavior of the nanotubes (Figure 8(a)) [25] with the estimated band gap of 1.5–2 V. In addition, the *I-U* test demonstrated a remarkable difference between the DC conductivity of samples (8–11) compared to that of the neat epoxy (Supplementary Information Fig. S8) and the pure INT pellet (Figure 8). It was observed that with addition of the polymer phase to the nanotubes, the semiconducting behavior, typical for the pure pellet, diminished and the insulating properties of the resin became more pronounced. The highest current (highest conductivity) values for the voltage range of −50 to 50 V were observed for sample 8 where a minor pressure of 0.8 MPa was used during sample preparation. For samples 9–11 the current fluctuated around the same values (see Table 1). Contrarily, it was observed that the recorded current for the cast sample 7 (Supplementary Information Fig. S8) is significantly reduced, compared with the compression molded samples 8–11.

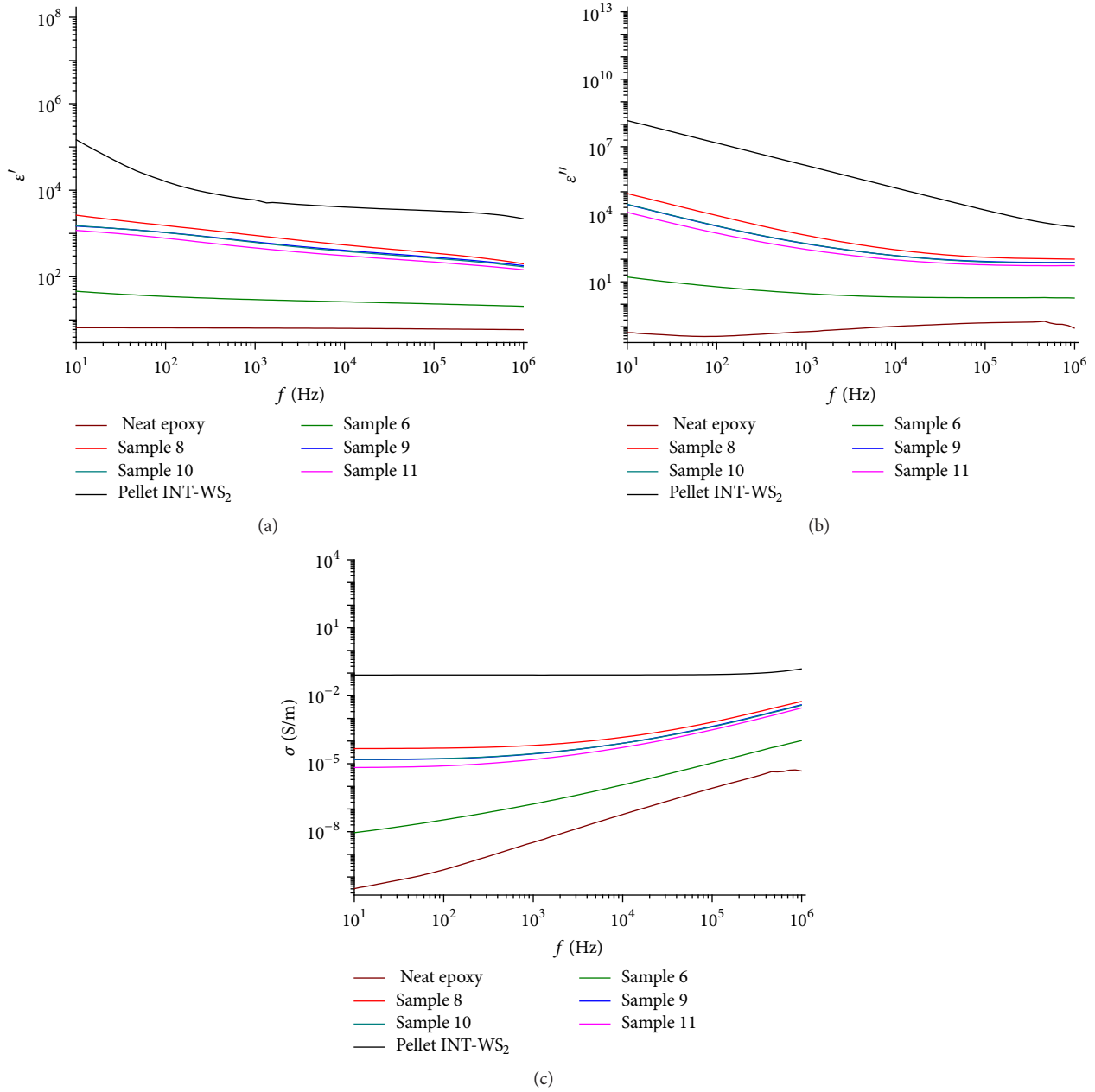

Figure 7: (a) Permittivity (dielectric constant-ε'), (b) imaginary permittivity (loss factor-ε''), and (c) AC conductivity (σ) versus frequency of the INT-WS_2 pellet, sample 6, samples 8–11, and the neat epoxy.

3.3. Relationships between DC Conductivity (σ) of Samples 8–11 and the Stress-Strain Relationship. The *I-U* characteristics (DC conductivity) and the impedance analysis of the samples indicated that only samples 8–11 (25 Vol.% of nanotubes) form continuous (conducting) nanotubes network. Therefore, these samples were chosen for the stress monitoring experiments. It was observed that a current stabilization period of 1.3–5 min is required (Supplementary Information Fig. S2) before applying load in the three-point bending configuration (Supplementary Information Fig. S1).

Conductivity measurements of samples containing INT-WS_2 (samples 8–11 with 25 Vol.% nanotubes) showed an increase in the current while applying the load (Figure 9(b)). In contrast to that, the neat epoxy did not show any change in conductivity with the applied load (Figure 9(a)). For all the tested samples the conductivity increased with the samples' strain. Initially the slope of the curves is rather moderate. Beyond a strain of $0.79 \pm 0.13\%$, the electrical response was enhanced, as can be observed from the steeper slope in Figure 9(b). In addition, the calculated sensitivity factors tend to be higher for the strain range of 1.0–1.3% (Table 2). In general, the sensitivity factors for sample 8 were found to be the highest among samples 8–11, in the strain range of 1.0–1.3%. It was observed that the maximum current increase

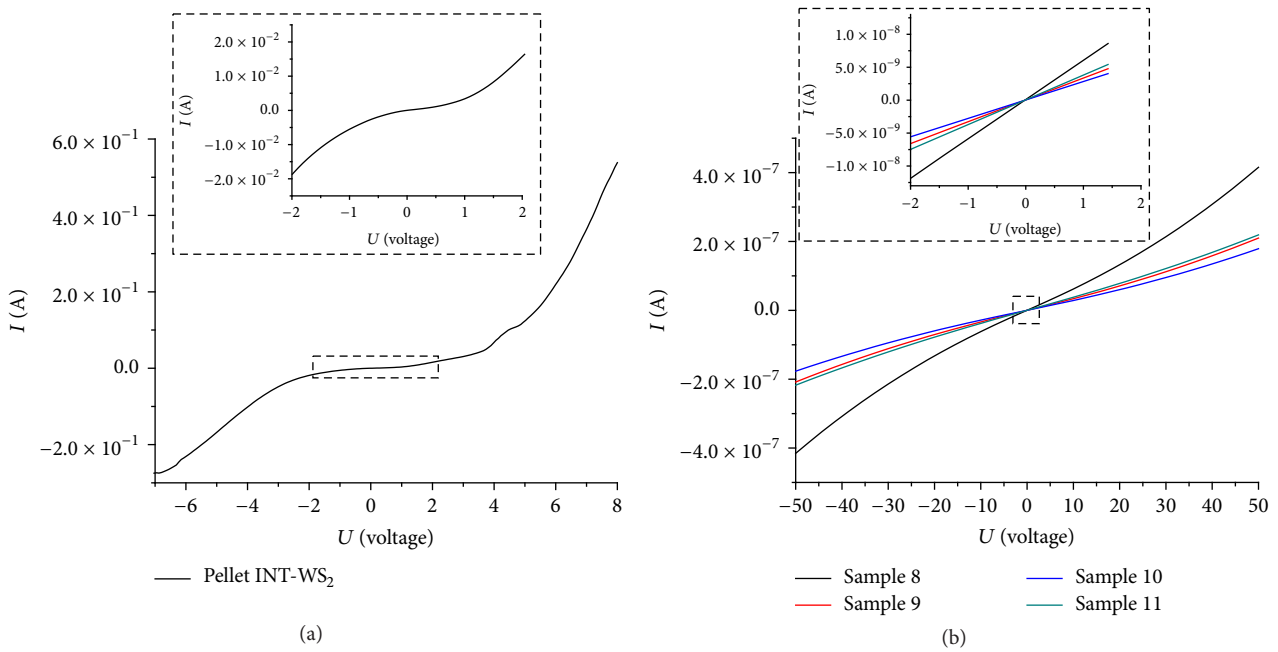

FIGURE 8: I-U relationship of the (a) pure INT-WS_2 compressed pellet and (b) samples 8–11.

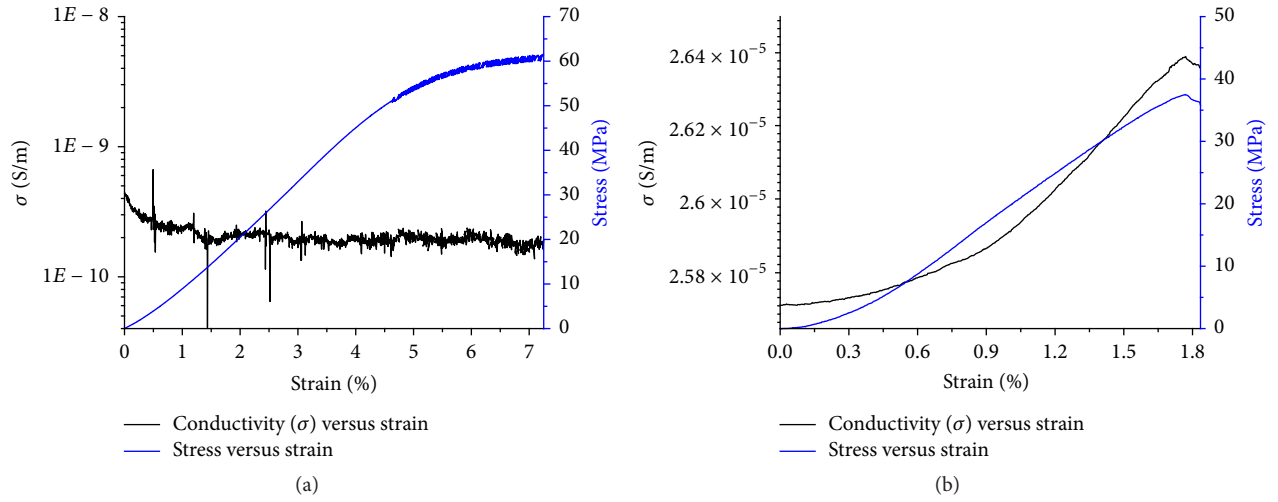

FIGURE 9: Conductivity versus strain (black curve) and the stress-strain relationship (blue curve) plots of the (a) neat epoxy and (b) sample 8.

due to the applied load for samples 8–11 is in the range of 2.0–2.7%. The current increase for sample 8 tends to be the highest (2.7%).

The content of the nanotubes in samples 8–11 is very high (25 Vol.%), which is appreciably higher than the range used for reinforcement of the resin (<2 Vol.%). Furthermore, the preparation methodology used for these samples did not allow proper dispersion of the nanotubes in the resin resulting in loosely attached nanotubes within the agglomerates (Figure 5(a)). Consequently, the mechanical properties of the epoxy-nanotubes composite in these samples were inferior to that of the pure epoxy (see Figures 9(a) and 9(b)), let alone the values obtained for nanotube reinforced resin. It was found that the maximum strain that these samples exhibit is only 20–23% of the neat epoxy strain (Table 2). It should be noted that the failure of individual WS_2 nanotube occurred at a maximum elongation of 5–14% [4, 46].

By analyzing the stress-strain/conductivities relationship of samples 8–11, it was found that the DC current increased (electrical resistance decrease) upon increasing the stress in the samples (Figure 9(b)). It was shown before that by applying tensile force on individual WS_2 nanotube using nanoelectromechanical devices a current increase is expected [26]. These results are also in agreement with theoretical study where structural modifications of the WS_2 nanotube and lowering of its bandgap are predicted due to the W-S

nanotube bond elongation (and angular distortion) through the tensile stress [24]. We assume that the main reason for the current increase in our sample is the tension of the individual nanotube due to an applied load in the three-point bending configuration. Additional reason for such phenomena could be the reorientation of the nanotubes' agglomerates under the applied load.

4. Conclusions

The electrical conductivity and the dielectric properties of the INT-WS_2/epoxy composites were studied. Accordingly, the possibility of the INT-WS_2 to serve as stress monitoring elements in the composites was evaluated. In order to analyze the percolating network formation, epoxy samples with various nanotubes content (samples 1–6) were prepared. These samples were analyzed using impedance measurements. It was observed that only samples containing as high as 6.2 Vol.% (sample 6) of the nanotubes could show significant enhancement of the dielectric properties compared to the neat epoxy. We assume that the nanotubes segregation observed in this sample has an influence on the dielectric properties enhancement.

Samples with high nanotubes content (25 Vol.%), which surpassed the percolation threshold, were prepared as well. A specially designed mold was fabricated allowing compression molding of the INT-WS_2/epoxy mixture using various pressures of 0.8, 13.9, 27.8, and 55.6 MPa (samples 8–11). Cast samples containing high volume fraction of the INT-WS_2, prepared without applied pressure but using thorough mixing which instigated a partial deagglomeration of the nanotubes aggregates (sample 7), were prepared as well. These samples exhibited low conductivity and poor dielectric properties. We believe that the nanotubes wrapping by the insulating polymer are the main reason for these results.

On the other hand, samples which were prepared under pressure, and light mixing only, showed appreciable conductivity. Thus, electrical conductivity on the order of 10^{-5} [S/m] was recorded for the epoxy samples containing high volume fraction of the INT-WS_2 (25 Vol.%, samples 8–11) compared to 10^{-10} (S/m) for the neat epoxy. SEM analysis of the fractured surfaces of the samples showed that, by applying compression pressures above a few MPa during the preparation of the specimens, the polymer is squeezed between the INT-WS_2 granules in higher amount and leads to deterioration of the overall specimens electrical conductivity. On the other hand, applying a moderate pressure (<1 MPa) during the samples' preparation resulted in higher conductivity values. This behavior was confirmed by the Nyquist plots.

Three-point bending loading with simultaneous current monitoring was performed on samples containing high (25 Vol.%) nanotubes content (samples 8–11) which surpassed the percolation threshold in epoxy resin. Using this configuration, the conductivity/stress-strain relation of the INT-WS_2/epoxy composites was obtained. In contrast to polymer compounded with CNTs, here the current was found to increase with the applied load. The increase in the current and the calculated sensitivity factors were appreciable (beyond 1 (or 100%), for the strain range of 1.0–1.3%).

Therefore, INT-WS_2 are suitable to serve as stress sensors in polymer-based composites due to their electrical response to the applied load and, consequently, to be applied in future stress monitoring applications and possibly also for electromagnetic shielding.

Conflicts of Interest

The authors declare that they have no conflicts of interest.

Acknowledgments

Special thanks are extended to Professor Igor Lubomirsky (Weizmann Institute) for the assistance with the impedance and DC conductivity characterization. This work was supported by the Israel National Nano-Initiative, the Israel Science Foundation, H. Perlman Foundation. The electron microscopy work was performed at the Irving and Cherna Moskowitz Center for Nano and BioNano Imaging (Weizmann Institute).

References

[1] W. Staszewski, C. Boller, and G. R. Tomlinson, *Health Monitoring of Aerospace Structures: Smart Sensor Technologies and Signal Processing*, John Wiley & Sons, 2004.

[2] G. Bartelds, "Aircraft structural health monitoring, prospects for smart solutions from a european viewpoint," *Journal of Intelligent Material Systems and Structures*, vol. 9, no. 11, pp. 906–910, 1998.

[3] S. Kim, S. Pakzad, D. Culler et al., "Health monitoring of civil infrastructures using wireless sensor networks," in *Proceedings of the 6th International Symposium on Information Processing in Sensor Networks (IPSN '07)*, pp. 254–263, IEEE, April 2007.

[4] I. Kaplan-Ashiri, S. R. Cohen, K. Gartsman et al., "On the mechanical behavior of WS_2 nanotubes under axial tension and compression," *Proceedings of the National Academy of Sciences of the United States of America*, vol. 103, no. 3, pp. 523–528, 2006.

[5] Y. Xiao, X. H. Yan, J. X. Cao, J. W. Ding, Y. L. Mao, and J. Xiang, "Specific heat and quantized thermal conductance of single-walled boron nitride nanotubes," *Physical Review B*, vol. 69, no. 20, Article ID 205415, 2004.

[6] T. W. Ebbesen, H. J. Lezec, H. Hiura, J. W. Bennett, H. F. Ghaemi, and T. Thio, "Electrical conductivity of individual carbon nanotubes," *Nature*, vol. 382, pp. 54–56, 1996.

[7] M. Naffakh, C. Marco, M. A. Gómez, J. Gómez-Herrero, and I. Jiménez, "Use of inorganic fullerene-like WS_2 to produce new high-performance polyphenylene sulfide nanocomposites: role of the nanoparticle concentration," *Journal of Physical Chemistry B*, vol. 113, no. 30, pp. 10104–10111, 2009.

[8] E. Zohar, S. Baruch, M. Shneider et al., "The effect of WS_2 nanotubes on the properties of epoxy-based nanocomposites," *Journal of Adhesion Science and Technology*, vol. 25, no. 13, pp. 1603–1617, 2011.

[9] C. Zhi, Y. Bando, T. Terao, C. Tang, H. Kuwahara, and D. Golberg, "Towards thermoconductive, electrically insulating polymeric composites with boron nitride nanotubes as fillers," *Advanced Functional Materials*, vol. 19, no. 12, pp. 1857–1862, 2009.

[10] S. G. Prolongo, G. Del Rosario, and A. Ureña, "Coupled thermal-electrical analysis of carbon nanotube/epoxy composites," *Polymer Engineering and Science*, vol. 54, no. 9, pp. 1976–1982, 2014.

[11] S. Iijima, "Helical microtubules of graphitic carbon," *Nature*, vol. 354, no. 6348, pp. 56–58, 1991.

[12] S. Iijima and T. Ichihashi, "Single-shell carbon nanotubes of 1-nm diameter," *Nature*, vol. 363, no. 6430, pp. 603–605, 1993.

[13] C. Stampfer, A. Jungen, R. Linderman, D. Obergfell, S. Roth, and C. Hierold, "Nano-electromechanical displacement sensing based on single-walled carbon nanotubes," *Nano Letters*, vol. 6, no. 7, pp. 1449–1453, 2006.

[14] E. D. Minot, Y. Yaish, V. Sazonova, J.-Y. Park, M. Brink, and P. L. McEuen, "Tuning carbon nanotube band gaps with strain," *Physical Review Letters*, vol. 90, no. 15, p. 156401, 2003.

[15] L. Yang, M. P. Anantram, J. Han, and J. P. Lu, "Band-gap change of carbon nanotubes: effect of small uniaxial and torsional strain," *Physical Review B*, vol. 60, no. 19, p. 13874, 1999.

[16] M. D. Rein, O. Breuer, and H. D. Wagner, "Sensors and sensitivity: carbon nanotube buckypaper films as strain sensing devices," *Composites Science and Technology*, vol. 71, no. 3, pp. 373–381, 2011.

[17] L. Böger, M. H. G. Wichmann, L. O. Meyer, and K. Schulte, "Load and health monitoring in glass fibre reinforced composites with an electrically conductive nanocomposite epoxy matrix," *Composites Science and Technology*, vol. 68, no. 7-8, pp. 1886–1894, 2008.

[18] E. T. Thostenson and T. W. Chou, "Carbon nanotube networks: sensing of distributed strain and damage for life prediction and self healing," *Advanced Materials*, vol. 18, no. 21, pp. 2837–2841, 2006.

[19] C. Li and T.-W. Chou, "Modeling of damage sensing in fiber composites using carbon nanotube networks," *Composites Science and Technology*, vol. 68, no. 15-16, pp. 3373–3379, 2008.

[20] N. Hu, Y. Karube, C. Yan, Z. Masuda, and H. Fukunaga, "Tunneling effect in a polymer/carbon nanotube nanocomposite strain sensor," *Acta Materialia*, vol. 56, no. 13, pp. 2929–2936, 2008.

[21] R. Tenne, L. Margulis, M. Genut, and G. Hodes, "Polyhedral and cylindrical structures of tungsten disulphide," *Nature*, vol. 360, no. 6403, pp. 444–446, 1992.

[22] L. Margulis, G. Salitra, R. Tenne, and M. Talianker, "Nested fullerene-like structures," *Nature*, vol. 365, no. 6442, pp. 113–114, 1993.

[23] D.-M. Tang, X. Wei, M.-S. Wang et al., "Revealing the anomalous tensile properties of WS_2 nanotubes by in situ transmission electron microscopy," *Nano Letters*, vol. 13, no. 3, pp. 1034–1040, 2013.

[24] N. Zibouche, M. Ghorbani-Asl, T. Heine, and A. Kuc, "Electromechanical properties of small transition-metal dichalcogenide nanotubes," *Inorganics*, vol. 2, no. 2, pp. 155–167, 2014.

[25] R. Levi, O. Bitton, G. Leitus, R. Tenne, and E. Joselevich, "Field-effect transistors based on WS_2 nanotubes with high current-carrying capacity," *Nano Letters*, vol. 13, no. 8, pp. 3736–3741, 2013.

[26] R. Levi, J. Garel, D. Teich, G. Seifert, R. Tenne, and E. Joselevich, "Nanotube electromechanics beyond carbon: the case of WS_2," *ACS Nano*, vol. 9, no. 12, pp. 12224–12232, 2015.

[27] F. Qin, W. Shi, T. Ideue et al., "Superconductivity in a chiral nanotube," *Nature Communications*, vol. 8, 2017.

[28] M. Naffakh and A. M. Díez-Pascual, "Nanocomposite biomaterials based on poly(ether-ether-ketone) (PEEK) and WS_2 inorganic nanotubes," *Journal of Materials Chemistry B*, vol. 2, no. 28, pp. 4509–4520, 2014.

[29] G. Otorgust, A. Sedova, H. Dodiuk, S. Kenig, and R. Tenne, "Carbon and tungsten disulfide nanotubes and fullerene-like nanostructures in thermoset adhesives: a critical review," *Reviews of Adhesion and Adhesives*, vol. 3, no. 3, pp. 311–363, 2015.

[30] E. Zohar, S. Baruch, M. Shneider et al., "The mechanical and tribological properties of epoxy nanocomposites with WS_2 nanotubes," *Sensors and Transducers*, vol. 12, pp. 53–65, 2011.

[31] A. Voldman, D. Zbaida, H. Cohen, G. Leitus, and R. Tenne, "A nanocomposite of polyaniline/inorganic nanotubes," *Macromolecular Chemistry and Physics*, vol. 214, no. 18, pp. 2007–2015, 2013.

[32] S. Kumar, C. Borriello, G. Nenna, R. Rosentsveig, and T. Di Luccio, "Dispersion of WS_2 nanotubes and nanoparticles into conducting polymer matrices for application as LED materials," *European Physical Journal B*, vol. 85, no. 5, article no. 160, pp. 1–7, 2012.

[33] Q. Li, Q. Xue, L. Hao, X. Gao, and Q. Zheng, "Large dielectric constant of the chemically functionalized carbon nanotube/polymer composites," *Composites Science and Technology*, vol. 68, no. 10-11, pp. 2290–2296, 2008.

[34] L. Wang and Z.-M. Dang, "Carbon nanotube composites with high dielectric constant at low percolation threshold," *Applied Physics Letters*, vol. 87, no. 4, Article ID 042903, 2005.

[35] P. Pötschke, S. M. Dudkin, and I. Alig, "Dielectric spectroscopy on melt processed polycarbonate—multiwalled carbon nanotube composites," *Polymer*, vol. 44, no. 17, pp. 5023–5030, 2003.

[36] J. Petzelt, D. Nuzhnyy, V. Bovtun, M. Savinov, M. Kempa, and I. Rychetsky, "Broadband dielectric and conductivity spectroscopy of inhomogeneous and composite conductors," *Physica Status Solidi (A) Applications and Materials Science*, vol. 210, no. 11, pp. 2259–2271, 2013.

[37] V. K. Ksenevich, N. I. Gorbachuk, H. Viet et al., "Electrical properties of carbon nanotubes/WS_2 nanotubes (nanoparticles) hybrid films," *Nanosystems: Physics, Chemistry, Mathematics*, vol. 7, no. 1, pp. 37–43, 2016.

[38] M. B. Heaney, "Electrical conductivity and resistivity," in *Meas. Instrum. sensorsHandb*, pp. 1332–1345, 2000.

[39] V. F. Lvovich, *Impedance Spectroscopy: Applications to Electrochemical and Dielectric Phenomena*, John Wiley & Sons, 2012.

[40] E. Barsoukov and J. R. Macdonald, *Impedance Spectroscopy: Theory, Experiment, and Applications*, John Wiley & Sons, 2005.

[41] A. Zak, L. S. Ecker, R. Efrati, L. Drangai, N. Fleischer, and R. Tenne, "Large-scale synthesis of WS_2 multiwall nanotubes and their dispersion, an update," *Sensors & Transducers*, vol. 12, p. 1, 2011.

[42] M. Krause, A. Mücklich, A. Zak, G. Seifert, and S. Gemming, "High resolution TEM study of WS_2 nanotubes," *Physica Status Solidi (B) Basic Research*, vol. 248, no. 11, pp. 2716–2719, 2011.

[43] M. Shneider, H. Dodiuk, R. Tenne, and S. Kenig, "Nanoinduced morphology and enhanced properties of epoxy containing tungsten disulfide nanoparticles," *Polymer Engineering and Science*, vol. 53, no. 12, pp. 2624–2632, 2013.

[44] G. R. Higson, "Recent advances in strain gauges," *Journal of Scientific Instruments*, vol. 41, no. 7, pp. 405–414, 1964.

[45] G. T. Pham, Y.-B. Park, Z. Liang, C. Zhang, and B. Wang, "Processing and modeling of conductive thermoplastic/carbon

nanotube films for strain sensing," *Composites Part B: Engineering*, vol. 39, no. 1, pp. 209–216, 2008.

[46] M. S. Wang, I. Kaplan-Ashiri, X. L. Wei et al., "In situ TEM measurements of the mechanical properties and behavior of WS_2 nanotubes," *Nano Research*, vol. 1, no. 1, pp. 22–31, 2008.